Research Article

MOLECULAR PAIN

Molecular Pain
Volume 15: 1–16

DOI: 10.1177/1744806918825044
journals.sagepub.com/home/mpx
SAGE

Altered glial glutamate transporter expression in descending circuitry and the emergence of pain chronicity

Wei Guo[1,2], Satoshi Imai[1,2], Shiping Zou[1,2], Jiale Yang[1,2], Mineo Watanabe[1,2,3], Jing Wang[1,2,4], Ronald Dubner[1,2], Feng Wei[1,2], and Ke Ren[1,2]

Abstract

Background: The glutamate type 1 transporter (GLT1) plays a major role in glutamate homeostasis in the brain. Although alterations of GLT1 activity have been linked to persistent pain, the significance of these changes is poorly understood. Focusing on the rostral ventromedial medulla, a key site in pain modulation, we examined the expression and function of GLT1 and related transcription factor kappa B-motif binding phosphoprotein (KBBP) in rats after adjuvant-induced hind paw inflammation.

Results: After inflammation, GLT1 and KBBP showed an early upregulation and gradual transition to downregulation that lasted throughout the eight-week observation period. Nitration of GLT1 was reduced at 30 min and increased at eight weeks after inflammation, suggesting an initial increase and later decrease in transporter activity. Mechanical hyperalgesia and paw edema exhibited an initial *developing* phase with peak hyperalgesia at 4 to 24 h, a subsequent *attenuating* phase, followed by a late *persistent* phase that lasted for months. The downregulation of GLT1 occurred at a time when hyperalgesia transitioned into the persistent phase. In the rostral ventromedial medulla, pharmacological block with dihydrokainic acid and RNAi of GLT1 and KBBP increased nociception and overexpression of GLT1 reversed persistent hyperalgesia. Further, the initial upregulation of GLT1 and KBBP was blocked by local anesthetic block, and pretreatment with dihydrokainic acid facilitated the development of hyperalgesia.

Conclusions: These results suggest that the initial increased GLT1 activity depends on injury input and serves to dampen the development of hyperalgesia. However, later downregulation of GLT1 fosters the net descending facilitation as injury persists, leading to the emergence of persistent pain.

Keywords

Glutamate transporter, kappa B-motif binding phosphoprotein, inflammation, rostral ventromedial medulla

Date Received: 29 November 2018; revised: 16 December 2018; accepted: 17 December 2018

Introduction

Pain is commonly associated with tissue or nerve injury. Although such pain may be transient, or acute, it may become chronic or persistent even when the injured body appears healed. Studies have pointed that, in addition to input generated from peripheral nociceptors, the transition of acute to chronic pain and the maintenance of pain hypersensitivity involves neuron–glial interactions and sensitization in the central nervous system.[1,2] Multiple cortical and brainstem regions are implicated in the development of chronic pain.[3,4] Notably, active descending facilitation from the periaqueductal gray (PAG)-rostral ventromedial medulla (RVM)-spinal pathways

[1]Department of Neural and Pain Sciences, School of Dentistry, University of Maryland, Baltimore, MD, USA
[2]Program in Neuroscience, University of Maryland, Baltimore, MD, USA
[3]Department of Oral Biology, Division of Molecular Medical Science, Hiroshima, Japan
[4]Key Laboratory of Bone and Joint Diseases of Gansu province, Institute of Orthopedics, the Second Hospital of Lanzhou University, Lanzhou, China

Corresponding Author:
Ke Ren, Department of Neural and Pain Sciences, 650 W. Baltimore St., Dental-8 South, Baltimore, MD 21201-1586, USA.
Email: kren@umaryland.edu

plays a major role in persistent pain.[5–7] The PAG receives convergent input from major pain-related rostral brain structures including prefrontal cortex,[8] insular cortex,[9] anterior cingulate cortex,[10] amygdala,[11,12] and hypothalamus.[8] The RVM relays input from the PAG to the spinal cord as well as receives direct ascending nociceptive information from the parabrachial complex[13] and has been considered pivotal in descending pain modulation.[14,15] Altered functional activity in the RVM after injury favors the development of persistent pain.[16–19]

Glutamate is the major excitatory amino acid neurotransmitter in the mammalian nervous system. After synaptic activation, glutamate is actively cleared from the synaptic cleft by excitatory amino acid transporters (EAAT), mainly glial glutamate transporters (GLTs). Efficient removal of synaptic glutamate maintains homeostasis for brain functions. Among a group of five EAATs,[20–22] the astroglia selective membrane glutamate type 1 transporter (GLT1, human homology EAAT2) is the predominant subtype responsible for maintaining a normal level of neuronal activity and a key player in reciprocal neuron–glial interactions that underlie a variety of neurological disorders.[23–25]

GLT activity has been linked to persistent pain conditions.[21,26] Rodent models of persistent pain are associated with a decrease in GLT1 activity[27–33] (but see Yaster et al).[34] Blocking GLT1 leads to an increase in N-methyl-D-aspartate (NMDA) receptor activation[35] and behavioral hyperalgesia.[36,37] In contrast, increasing spinal GLT1 expression alleviates neuropathic pain behavior and suppresses glial activation[38] and attenuates visceral nociception.[39]

Although studies have documented alterations of GLTs in persistent pain, the significance of these changes is poorly understood. A key question remains to be answered is whether their activity contributes to the central mechanisms of transition to chronic pain. Focusing on the RVM, we carefully compared the time course of GLT1 modulation and behavioral hyperalgesia following complete Freund's adjuvant (CFA)-induced hind paw inflammation and tested the effect of altered GLT1 expression on pain behavior during different phases of hyperalgesia. To understand the cellular mechanisms of GLT1 regulation, we also studied an upstream modulator of GLT1, kappa B-motif binding phosphoprotein (KBBP)[25] in the CFA model. Advancing from previous studies, our results suggest that time-dependent alterations of GLT1 activity in the RVM contribute to the emergence of lasting pain after injury.

Material and methods

Animals

Adult male Sprague–Dawley rats (Envigo-Harlan), ≈eight-week-old at the time of inoculation were used in all experiments. Rats were on a 12-h light/dark cycle and received food and water ad libitum. To produce inflammation and hyperalgesia, CFA (0.05 ml, Sigma) suspended in an oil:saline (1:1) emulsion was injected subcutaneously into the lateral plantar surface of one (behavioral and immunocytochemical studies) or two (Western blot studies) hind paws. The CFA injection produced an intense tissue inflammation of the hind paw characterized by erythema, edema, and hyperalgesia.[40–42] Since we were not studying the effect of adjuvant per se and vehicle injection may also produce an effect,[43,44] we used naïve animals as a control. The animals were housed in cages in which the floor was covered with soft bedding materials to minimize discomfort due to contact with a cold, hard surface. The inflamed animals groom normally and display normal locomotor activity. They maintain their weight, explore their environment, and interact with other rats. The behavioral studies involved stimulation that produced only momentary pain and the rats could escape from these stimuli at any time. The experiments were approved by the Institutional Animal Care and Use Committee of the University of Maryland School of Dentistry.

Behavioral testing

All behavioral tests were conducted under blind conditions. For thermal nocifensive responses, rats were placed in clear plastic chambers on an elevated table and allowed to acclimate for approximately 15 to 30 min. Thermal hyperalgesia was assessed by measuring the latency of paw withdrawal in response to a radiant heat source.[45] The heat stimulus was applied from underneath the glass floor with a high-intensity projector lamp bulb (8 V, 50 W; Osram, Berlin, Germany) and focused on the plantar surface of the hind paw. The paw withdrawal latency (PWL) was determined by an electronic clock circuit. A 20-s cutoff was used to prevent tissue damage. The PWL was tested for three trials with 5-min intervals between each trial. The average of the three trials was then used for analysis.

For mechanical sensitivity, an electronic von Frey unit (EVF3, Bioseb) was used to deliver mechanical stimulation. The measurement range of the unit is 0 to 500 g with 0.1 g resolution. The hind paw skin was accessed through a dorsal approach as described previously[46] except that an electronic von Frey probe was used. The probe was applied against the lateral edge of the hind paw with gradually increasing force. The force (g) that induced paw withdrawal was digitized by the unit and used as the threshold for mechanical nociception.

For assessing conditioned place avoidance (CPA) behavior,[47,48] animals were placed within a $40.5 \times 30.5 \times 16$ cm Plexiglas chamber positioned on

top of a mesh screen. One half of the chamber was painted white (light area) and the other half was painted black (dark area). During CPA behavior testing, animals were allowed unrestricted movement throughout the test chamber for the duration of a 30-min test period. Testing began immediately with a suprathreshold mechanical stimulus (758 mN von Frey monofilament) applied abruptly to the hind paw at 15-s intervals. The stimulus was applied to the CFA-injected paw when the animal was within the preferred dark area and to the non-injected side when the animal was within the non-preferred light area. Based on the location of the animal at each 15-s interval, the mean percentage of time spent in each side of the chamber was calculated for the entire test period. Rats normally prefer to stay in the dark area. However, if staying in the preferred dark side was associated with a painful and aversive stimulus, the rat was forced to decide to remain there or to go to the light area to avoid the painful stimulus. The tendency to move to and stay in the light area is a measure of the aversion of the stimulus. CFA induces an increase in time spent in the light area. Spending less time in the light area of the chamber would suggest reduced aversive behavior.

Paw thickness (mm) was measured with a digital caliper to assess edema after CFA.

Brainstem microinjections and targeted recombinant plasmid transfers by electroporation[49]

Rats were anesthetized with 2% to 3% isoflurane in a gas mixture of 30% O_2 balanced with 70% nitrogen and placed in a Kopf stereotaxic instrument (Mode 900, Kopf Instruments, Tujunga, CA). A midline incision was made after infiltration of lidocaine (2%) into the skin. A midline opening was made in the skull with a dental drill for inserting an injection needle into the target site. The coordinates for the RVM were as follows: 10.5 mm caudal to bregma, midline, and 9.0 mm ventral to the surface of the cerebellum.[50] To avoid penetration of the transverse sinus, the incisor bar was set at 4.7 mm below the horizontal plane passing through the interaural line. Animals were subsequently maintained at ~1% isoflurane. Microinjections (500 nl) were performed by delivering drug solutions slowly over a 10-min period using a Hamilton syringe with a 32-gauge needle. The sham group underwent identical procedures with the injection of the same volume of the vehicle.

For gene transfer, Suresilencing™ shRNA plasmids with green fluorescent protein (GFP) (SAB Bioscience) were used. The shRNA inserts are: GCAAGCG CTAAGAGAGTTCTT (GLT1), CTAGTAACT TGGCATCTGTAT (KBBP2), and GGAATCTCATT CGATGCATAC (scrambled control). For GLT1 overexpression, we transfected RVM with GLT1 plasmid with GFP expression (PcDNA3.1/Hrgro_GLT1 cloning site BAMH I and XhoI, Gift from Dr. J. Rothstein), and vectors without GLT1 were used as a control. Each vector (500 ng/500 nl) was firstly injected into the RVM. The injection needle was left in place for at least 15 min before being slowly withdrawn. A pair of Teflon coated silver positive and negative electrodes were placed along a line rostral and caudal to the injection site. For transfer of negatively charged plasmid into RVM neurons, seven square wave electric pulses (40 V, 50 ms, 1 Hz; model 2100; A-M Systems, Carlsborg, WA) were delivered.[51] All wound margins were covered with a local anesthetic ointment (Nupercainal; Rugby Laboratories), the wound was closed, and animals were returned to their cages after they recovered from anesthesia. Following behavioral testing, animals were anesthetized with pentobarbital and perfused with saline and 4% paraformaldehyde. Coronal sections (60 μm) of tissue sections stained with cresyl violet were examined to determine needle placement.

Western blot

The rats were anesthetized with isoflurane (3%) and quickly decapitated. A block of brainstem from post interaural line 1.3 mm to 2.5 mm was punched out and put immediately into dry ice. RVM tissues from the ventral half and middle portion of the rostral medulla[50] were punched with a 15-gauge puncture needle. The tissues were homogenized in solubilization buffer (50 mM Tris.HCl, pH 8.0; 150 mM NaCl, 1 mM EDTA, 1% NP40, 0.5% deoxycholic acid, 0.1% sodium dodecyl sulfate (SDS), 1 mM Na_3VO_4, 1 U/ml aprotinin, 20 μg/ml leupetin, and 20 μg/ml pepstatin A). The homogenate was centrifuged at 20,200 *g* for 10 min at 4°C. The supernatant was removed. The protein concentration was determined using a detergent-compatible protein assay with a bovine serum albumin standard. Each sample contains proteins from one animal. The proteins (50 μg) were separated on a 4% to 20% SDS-polyacrylamide gel electrophoresis (PAGE) (Bio-Rad) and blotted to a nitrocellulose membrane (Amersham Biosciences). The blots were blocked with 5% milk in tris-buffered saline (TBS) buffer and then incubated with respective antibodies. The membrane was washed with TBS and incubated with horseradish peroxidase-linked secondary antibody. The immunoreactivity was detected using enhanced chemiluminescence (ECL, Amersham). In some experiments, the immunoreactivity was detected with near-infrared fluorescence. For the Odyssey Infrared Imaging System, 50 μg protein samples were denatured by boiling for 5 min and loaded onto 4% to 20% Bis-Tris gels (Invitrogene). After electrophoresis, proteins were transferred to nitrocellulose membranes.

The membranes were blocked for 1 h with Odyssey Blocking Buffer and then incubated with primary antibodies diluted in Odyssey Blocking Buffer at 4°C overnight, followed by washing with phosphate-buffered saline (PBS) containing 0.1% Tween 20 (PBST) three times. The membranes were then incubated for 1 h with IRDye800CW-conjugated goat anti-rabbit IgG and IRDye680-conjugated goat anti-mouse IgG secondary antibodies (LI-COR Biosciences) diluted in Odyssey Blocking Buffer. The blots were further washed three times with PBST and rinsed with PBS. Proteins were visualized by scanning the membrane with 700- and 800-nm channels (Odyssey®CLx, LI-COR Biosciences). β-actin was used as a loading control.

Immunoprecipitation

Samples were incubated with anti-GLT1 antibody overnight and then with protein A/G-Sepharose beads (Santa Cruz Biotechnology). SDS sample buffer (0.05 ml) was added to elute proteins from the protein A/G beads. The eluant was separated on SDS-PAGE (7.5%) and transferred to a nitrocellulose membrane. The membranes were blocked and incubated with anti-nitrotyrosine antibody, further washed and incubated with anti-mouse IgG horseradish peroxidase (1:3,000), and ECL was performed. The membranes were then stripped and reprobed with anti-GLT1 antiserum.

Immunohistochemistry

Rats were deeply anesthetized with pentobarbital sodium (100 mg/kg, i.p.) and perfused transcardially with 4% paraformaldehyde in 0.1 M phosphate buffer at pH 7.4. The same block of caudal brainstem tissues as that for western blot was removed, post-fixed, and transferred to 25% sucrose (w/v) for cryoprotection. Free-floating tissue sections were incubated with relevant antibodies with 1% to 3% relevant normal sera, and single or double-labeling immunofluorescence was performed. Double-labeling immunofluorescence was performed with the secondary antibodies labeled with Cy2 (1:500, Jackson ImmunoResearch) or Alexa Fluor 488 (1:500, Invitrogen Molecular Probes) and Cy3 (1:500, Jackson ImmunoResearch) after incubation with respective primary antibodies. Control sections were processed with the same method except that the primary antisera are omitted or adsorbed by respective antigens.

Antibodies and drugs

The following reagents were purchased: mouse anti-rat GLT1/EAAT2 antibody (1:1,000, BD Transduction Laboratories), mouse anti-heterogeneous nuclear ribonucleoproteins (hnRNP)/KBBP2 antibody (1:2,000, Santa Cruz Biotechnology), rabbit anti-GLAST (EAAT1, 1:1,000, Alpha Diagnostic Intl), rabbit anti-EAAC1: neuronal glutamate transporter (EAAT3, 1:1,000, BD Transduction Laboratories); Rabbit anti-gamma-aminobutyric acid (GABA) Transporter 3 (GAT3, 1:1,000, EMD Millipore), rabbit anti-phospho-44/42 MAP kinase (Thr202/Thr204, 1:1,000, Cell Signaling), mouse anti-glial fibrillary acidic protein (GFAP, 1:2,000, Millipore), mouse anti-NeuN (1:1,000, Millipore), rabbit anti-GFP (1:1,000, Millipore), mouse anti-nitrotyrosine antibody (1:1,000, EMD Millipore), mouse anti-β-actin (1:3,000, Sigma-Aldrich), PD98059 (Mol wt: 267.28, Calbiochem), dihydrokainic acid (DHK, Mol wt: 215.25, Sigma-Aldrich), and morphine sulphate (Mol Wt: 758.83, Sigma-Aldrich). The drugs were dissolved in saline or 5% dimethyl sulfoxide (Sigma) and saline. The drug vehicle was used as a control. The doses of all agents were selected based on previous use in relevant studies.

Data analysis

Data are presented as mean ± S.E.M. For Western blot analysis, the images were digitized, and densitometric quantification of immunoreactive bands was carried out using UN-SCAN-IT gel (ver. 4.3, Silk Scientific Inc.). The relative protein levels were obtained by comparing the respective specific band to the β-actin control from the same membrane. The deduced ratios were further normalized to that of the naïve rats on the same membrane and illustrated as percentage of the naïve controls. Statistical comparisons were made by analysis of variance (ANOVA) followed by post hoc comparisons with Bonferroni corrections. For the animals that are subject to repeated testing, ANOVA with repeated measures is used with time as a within-animal effect. $p \leq 0.05$ is considered significant for all cases.

Results

Altered GLT1 expression in the RVM after hind paw inflammation

We first examined whether GLT1 expression altered in the RVM after CFA-induced hind paw inflammation. Total proteins from RVM tissues were isolated and separated. The GLT1 antibody recognizes one monomer band (≈ 65 kDa) and two oligomer (dimer and trimer) bands (Supplemental Figure 1).[22,52,53] Since GLT1 functions in the dimerized form,[20,38] we analyzed GLT1 dimer expression. As shown in Figure 1(a), GLT1 expression in the RVM exhibited biphasic changes after CFA. Compared to naïve animals, GLT1 was significantly increased initially at 30 min and gradually transitioned to downregulation after CFA. Downregulation of GLT1 reached significance at the two-week time point

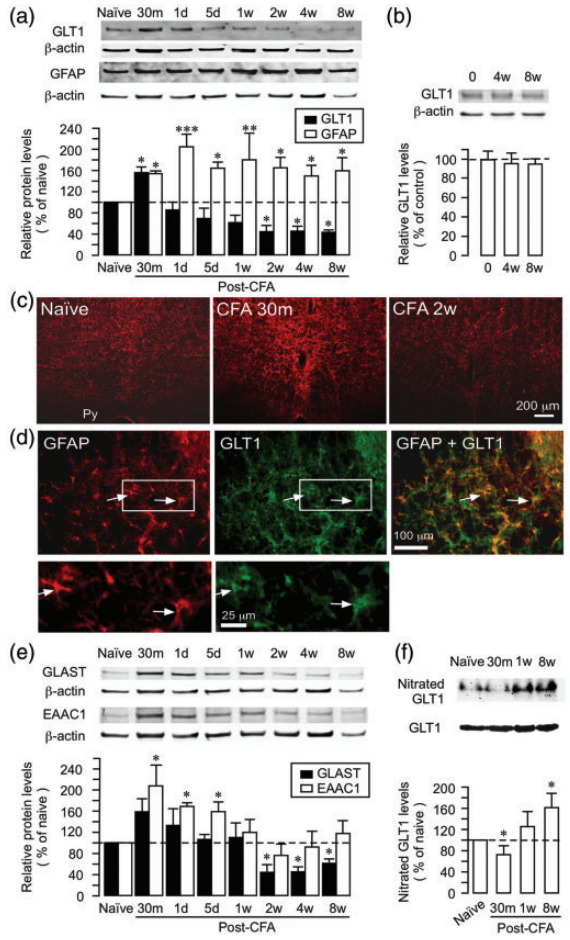

Figure 1. Altered glutamate transporter expression and GLT1 nitration in the RVM after hind paw inflammation. (a) Western immunoblot illustrating CFA-induced changes in dimerized GLT1 and GFAP expression. The RVM tissues were punched out at 30 min to eight weeks after CFA injection. Examples of the blot are shown on top and the relative protein levels are shown in the bottom histogram. Dashed line indicates the naïve level. The immunobands against β-actin were a loading control. (b) GLT1 expression in naïve rats over the same period as in (a). N = 4. (c) GLT1 immunostaining in the RVM. Py, pyramidal tract. (d) Double immunofluorescence labeling of GLT1 and GFAP illustrating astroglial localization of GLT1. Arrows indicate examples of GFAP and GLT1-labeled cells. The area in rectangles in top left and middle panels are enlarged below. (e) CFA-induced changes in GLAST and EAAC1 expression. *$p < 0.05$; **$p < 0.01$; ***$p < 0.001$ vs. naïve. N = 4 for each group. (f) CFA-induced changes in GLT-nitration. *$p < 0.05$ vs. naïve, N = 4. Error bars represent S.E.M. GLT1: glutamate type 1 transporter; GFAP: glial fibrillary acidic protein; CFA: complete Freund's adjuvant.

and remained at the significantly lower level throughout the eight-week observation period ($p < 0.05$). In naïve rats, GLT1 expression was not changed over the same period (Figure 1(b)), excluding an effect of other non-specific factors or aging on GLT1 expression.

Immunostaining with anti-GLT1 antibodies confirmed biphasic changes of GLT1 after CFA (Figure 1 (c)) and colocalization of GLT1 with GFAP, an astroglial marker (Figure 1(d)). It is known that GLT1 expression does not mirror the level of GFAP.[54] In contrast to GLT1, GFAP expression in the RVM was constantly upregulated during the eight-week observation period after inflammation (Figure 1(a)). The prolonged reactive astrocytosis indicates that downregulation of GLT1 is not due to loss or silence of local astrocytes. The other major glial EAAT, GLAST (EAAT1) showed a trend to increase at 30 min and transitioned to downregulation at two to eight weeks after CFA (Figure 1(e)). The neuronal glutamate transporter EAAC1 (EAAT3) showed upregulation at 30 min to five days after inflammation and returned to and maintained at the control level after one to two weeks (Figure 1(e)).

Reduced GLT1 activity is associated with its nitration by peroxynitrite.[55,56] Utilizing GLT1 immunoprecipitation and an anti-nitrotyrosine antibody, GLT1 nitration in the RVM showed a reduction at 30 min, no significant change at one week, and an increase at eight weeks after CFA ($p < 0.05$) (Figure 1(f)). Thus, the levels of GLT1 nitration showed an opposite pattern to GLT1, suggesting an initial transient increase and later decrease in GLT1 transporter activity after inflammation.

Re-evaluation of CFA-induced behavioral hyperalgesia

CFA-induced thermal hyperalgesia resolves in about two to four weeks[40] (Figure 2(a)). We noticed that the downregulation of GLT1 occurred at a time when thermal pain hypersensitivity had started to attenuate or resolve. This seems to be against the hypothesis that reduced uptake of synaptic glutamate transmitter, as a result of GLT1 downregulation, leads to persistent neuronal hyperexcitability and hyperalgesia. We have performed experiments to address this apparent discrepancy.

Noting that CFA-induced mechanical hyperalgesia does not resolve as late as 3 weeks after inflammation,[46] we directly compared the time courses of CFA-induced thermal and mechanical pain hypersensitivity up to 13 weeks after CFA. Consistent with the previous results,[40] thermal hyperalgesia, indicated by shortened paw withdrawal latencies to a noxious heat stimulus, peaked at one day, started to attenuate at two days, and gradually resolved after about four weeks after CFA (Figure 2(a)). Mechanical allodynia/hyperalgesia showed a similar time course in the first three weeks as thermal hyperalgesia. However, mechanical hyperalgesia did not further attenuate from 2- to 3-week time point but persisted at a constant level throughout the 13-week observation period (Figure 2(b)). Thus, mechanical hyperalgesia exhibited initial *developing* (2 h to one day) and subsequent *attenuating* (three days to two weeks) phases and a late persistent phase (>two to

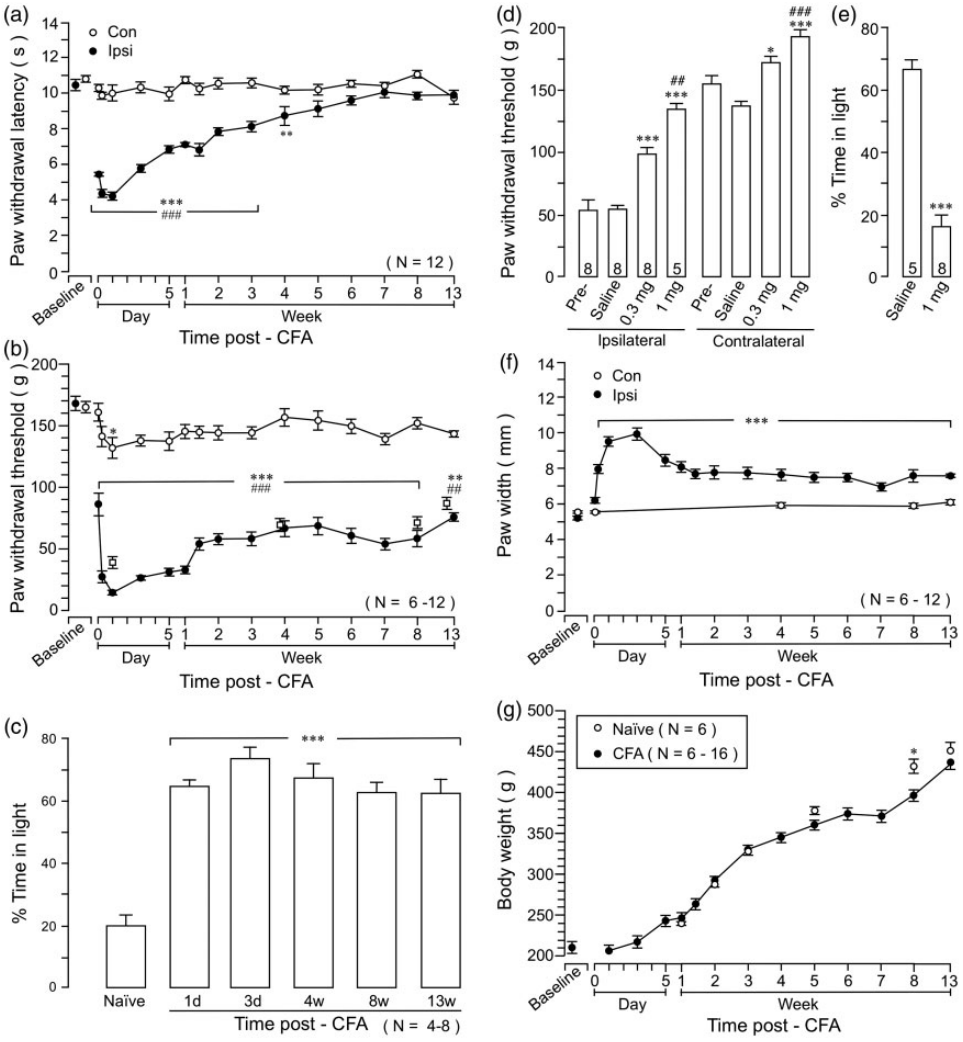

Figure 2. The time course of CFA-induced behavioral nociception. (a) Thermal hyperalgesia assessed with paw withdrawal responses to a noxious heat stimulus. (b) Mechanical hyperalgesia assessed with paw withdrawal threshold with an electronic von Frey probe. Open squares show PW threshold of a group of rats tested at longer intervals ($N = 6$). (a) and (b): $^{*}p < 0.05$; $^{**}p < 0.01$; $^{***}p < 0.001$ vs. baseline; $^{\#\#}p < 0.01$; $^{\#\#\#\#}p < 0.001$ vs. Contralateral. (c) The persistent pain hypersensitivity after CFA-induced inflammation was verified in a conditional place avoidance behavior test. Inflamed animals spend significantly more time in the light side of the chamber as compared to naïve rats, suggesting increased aversion, or negative affect, to the noxious stimulus. $^{***}p < 0.001$ vs. naïve. (d) The effects of morphine on long-lasting mechanical hyperalgesia. Morphine was injected i.p. at eight weeks after the injection of CFA (0.3 and 1 mg/kg, in 0.5 ml saline). Paw withdrawal threshold of the hind paw was significantly increased in both inflamed and non-inflamed paws at 45 to 60 min after the injection. $^{*}p < 0.05$; $^{***}p < 0.001$ vs. saline; $^{\#\#}p < 0.01$; $^{\#\#\#\#}p < 0.001$ vs. 0.3 mg. $N = 5$–8. (e) Compared to saline, morphine (1 mg/kg) significantly reduced time spent in the light area of the testing chamber in the CPA behavior test, suggesting suppression of aversion. $^{***}p < 0.001$ vs. saline. $N = 5$–8. (f) Hind paw edema, as measured by the paw thickness, followed a similar course as behavioral hyperalgesia. $^{***}p < 0.001$ vs. baseline. (g) Comparison of body weight between CFA-injected and naïve rats. Naïve rats were weighed at the matching age points with CFA rats. $^{*}p < 0.05$. CFA: complete Freund's adjuvant.

four weeks) after inflammation. To exclude a possible sensitization of mechanical responses due to repeated testing, a group of rats was tested at longer intervals ($N = 6$). Similar long-lasting mechanical hyperalgesia was observed in rats receiving fewer tests (Figure 2(b), open squares). There was a trend of reduced PW threshold on the contralateral non-inflamed paw, although it only reached statistical significance at the one-day time point (Figure 2(b)). The late long-lasting behavioral nociception after CFA was sensitive to analgesics. At eight weeks after inflammation, morphine (0.3 and 1 mg/kg, i.p., $p < 0.01$) increased paw withdrawal threshold (PWT), indicating attenuation of hyperalgesia (Figure 2(d)).

The CFA-induced lasting pain hypersensitivity was also assessed with the CPA behavior test in separate sets of animals. As shown in Figure 2(c), naïve rats tended to avoid staying in the light area of the test

chamber. They only spent a total of 20% ± 3% time in the light chamber. However, after receiving CFA, they spent over 60% of time in the light chamber ($p < 0.001$), indicating CFA-induced aversive behavior or pain affect. Different from mechanical hyperalgesia, there was no quantifiable difference in the magnitude of CPA behavior after CFA throughout the observation period. Morphine (1 mg/kg, i.p., $p < 0.001$) improved CPA behavior tested at eight weeks after inflammation (Figure 2(e)).

The paw edema as indicated by the paw thickness showed a time course similar to that of mechanical sensitivity with initial *developing*/*attenuating* phases and a late persistent phase (Figure 2(f)). CFA did not affect general growth assessed with body weight (Figure 2(g)). Compared to naïve rats, CFA-injected rats only showed reduced body weight at the 8-week time point during the 13-week period, suggesting that CFA did not have a general effect on the body.

Taken together, these results indicate that CFA-induced downregulation of GLT1 coincided with the emergence of the long-lasting pain hypersensitivity in the CFA model.

Altered GLT1 on pain sensitivity

We next examined whether inhibition of GLT1 in the RVM affect pain sensitivity. We first tested the effect of dihydrokainate (DHK), a GLT1 selective antagonist/glutamate uptake inhibitor. In naïve rats, intra-RVM injection (Figure 3(a)) of DHK (10 ng) produced a reduction of PWL in both hind paws (Figure 3(b)). Importantly, when injected at seven days after CFA when the GLT1 level and nitration were not significantly different from the naïve level (Figure 1(a) and (b)), DHK further reduced PWL on the inflamed paw and produced thermal hyperalgesia on the contralateral paw (Figure 3(c)).

We then focally knocked down GLT1 expression by RNAi in the RVM to mimic the tissue injury-induced reduction of GLT1 and examined its effect on nociception in normal animals. GLT1 shRNA plasmid was injected into the rat RVM and then effectively transferred into RVM cells by local electroporation. The same amount of unmatched shRNA plasmid was used as a control. Significant downregulation of GLT1 expression in the RVM was observed from one to five days after gene transfer, compared with the negative control shRNA (Figure 4(a) and (b)). Compared with the rats receiving control plasmid, GLT1 shRNA-treated animals showed significant decreases in PWLs (Figure 4(c)) and mechanical response threshold (Figure 4(d)) on both hind paws at one to seven days after gene transfer, indicating behavioral hyperalgesia. The pain hypersensitivity returned to the baseline level

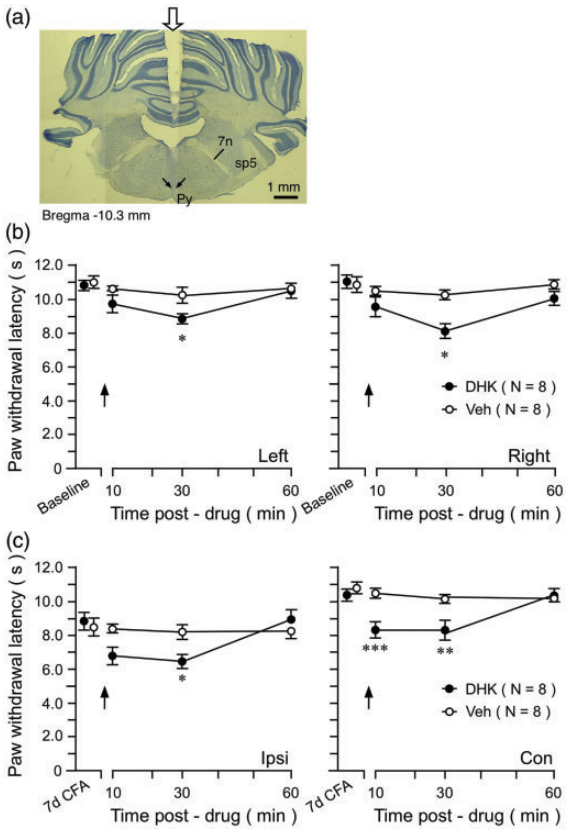

Figure 3. The effect of the GLT1 inhibitor on pain sensitivity. (a) Digital photomicrograph illustrating the site of microinjection in the RVM. The transverse section of the brainstem was taken at 10.30 mm posterior to the bregma. The start of penetration of the guide cannula is indicated by a block down arrow on top (middle). The tip of the microinjection needle is indicated by two small arrows dorsal to the pyramidal tract (py). 7, facial nerve; sp5, spinal trigeminal tract. (b) Intra-RVM injection of DHK reduced PWLs on both hind paws at 30 min after DHK injection in naïve rats. (c) At seven-day post-CFA, intra-RVM DHK further reduced PWL of the ipsilateral inflamed paw and induced hyperalgesia on the contralateral paw. *$p < 0.05$; **$p < 0.01$; ***$p < 0.001$ vs. Veh. DHK: dihydrokainic acid; CFA: complete Freund's adjuvant.

at 10 days after gene transfer. These results indicate that GLT1 activity in descending circuitry is involved in the modulation of nociceptive sensitivity.

The effect of GLT1 overexpression on hyperalgesia

We next tested whether induced-GLT1 overexpression could reverse persistent phase hyperalgesia. At four weeks after the injection of CFA, GFP-GLT1 plasmid was transfected into the RVM through microinjection followed by electroporation. GFP-GLT1 expression was predominantly in GFAP-labeled astrocytes (Figure 5a (a–d)) but not in neurons (not shown). While thermal hyperalgesia was small in magnitude at this point, induced GLT1 expression led to an increase in PWLs in both hind paws after gene transfer

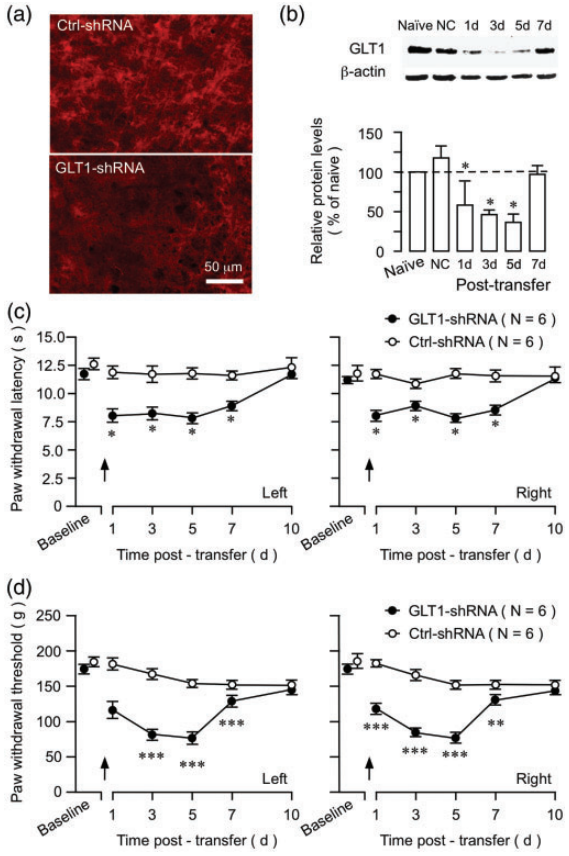

Figure 4. The effect of GLT1 knock down on nociception. (a) Tissue sections from the RVM were processed for GLT1 immunoreactivity from a rat receiving negative control shRNA (top) and a rat at three days after transfer of shRNA against GLT1 mRNA (bottom). Compared to the rat receiving negative control gene transfer, the GLT1 immunoreactivity was decreased in the RVM after the transfer of shRNA against GLT1 mRNA. (b) The GLT1 protein levels in the RVM were downregulated from one to five days and recovered at seven days after transfer of shRNA for GLT1 to the naïve rats. NC shRNA. *$p < 0.05$ vs. naïve. $N = 4$. (c) Both left and right PWLs were significantly decreased at one to seven days after the transfer of shRNA against GLT1 mRNA, compared to rats receiving negative control-shRNA (*$p < 0.05$ vs. Ctrl-shRNA). (d) The intra-RVM transfer of GLT1 shRNA decreased PW threshold of both paws. (c) and (d) Arrows indicate the gene transfection by electroporation. *$p < 0.05$; **$p < 0.01$; ***$p < 0.001$ vs. Ctrl-shRNA. GLT1: glutamate type 1 transporter; NC: negative control.

(Figure 5(b), left). GLT1 overexpression also led to an increased mechanical response threshold on both hind paws (Figure 5(b), right). Notably, thermal and mechanical hyperalgesia on the inflamed paw were reversed (Figure 5(b)). These results provide behavioral evidence that downregulation of GLT1 expression in the RVM contributes to decreased descending pain inhibition or increased descending facilitation that led to the development of persistent pain.

Altered KBBP expression after hind paw inflammation

KBBP is a transcription factor that regulates GLT1 expression by binding to an essential element of the GLT1 promoter.[25] We reasoned that KBBP expression would be similarly modulated by inflammation. We examined expression of KBBP in the RVM after hind paw inflammation. Western blot showed that KBBP expression was increased at 30 min to five days and returned to the baseline level at one week after injection of CFA (Figure 6(a)). Significant downregulation of KBBP was observed at two to eight weeks after inflammation ($p < 0.05$). Immunostaining of KBBP also showed an initial increase and later decrease of KBBP expression in the RVM (Figure 6(b)).

Similar upregulation of KBBP and GLT1 at the early 30-min time point prompted us to directly test whether KBBP contributed to CFA-induced GLT1. We injected shRNA against KBBP or negative control plasmid (1 μg) into the RVM, followed by electroporation. The treatment with KBBP shRNA reduced KBBP in the RVM at three to five days after transfection (Figure 6(c)). The control plasmid did not have an effect on KBBP expression. At three days after KBBP shRNA injection, CFA was injected into the hind paw. Both KBBP and GLT1 levels were unchanged at 30 min after CFA in KBBP shRNA-treated rats, while the control rats showed upregulation of KBBP and GLT1 (Figure 6(d) and (e)). Finally, the intra-RVM transfer of shRNA against KBBP mRNA produced pain hypersensitivity in naïve rats. PWT of both left and right hind paws was significantly decreased after the transfer of KBBP shRNA compared to rats receiving control plasmid (Figure 6 (f)). These results suggest that KBBP regulates GLT1 expression after peripheral tissue injury and that KBBP-GLT1 activity contributes to descending pain modulation.

Initial upregulation of GLT1 contributes to delayed descending facilitation after inflammation

What is the functional significance of initial increase in GLT1 expression and activity after peripheral tissue injury? The upregulation of GLT1 and decreased GLT1 nitration occurred as early as 30 min after the injection of CFA (Figure 1(a) and (b)), which is consistent with neuronal input-dependent GLT1 activation.[25,57] KBBP was also upregulated at 30 min after CFA (Figures 6 (a) and 7(a)). To examine a role of injury-related afferent input in altered GLT1 expression, a local anesthetic lidocaine (2%, 0.3 ml) was injected subcutaneously into the rat hind paw prior to the injection of CFA.[58] Ten minutes after the infiltration of lidocaine, CFA was injected into the same site. Compared to saline-treated rats, pretreatment with lidocaine

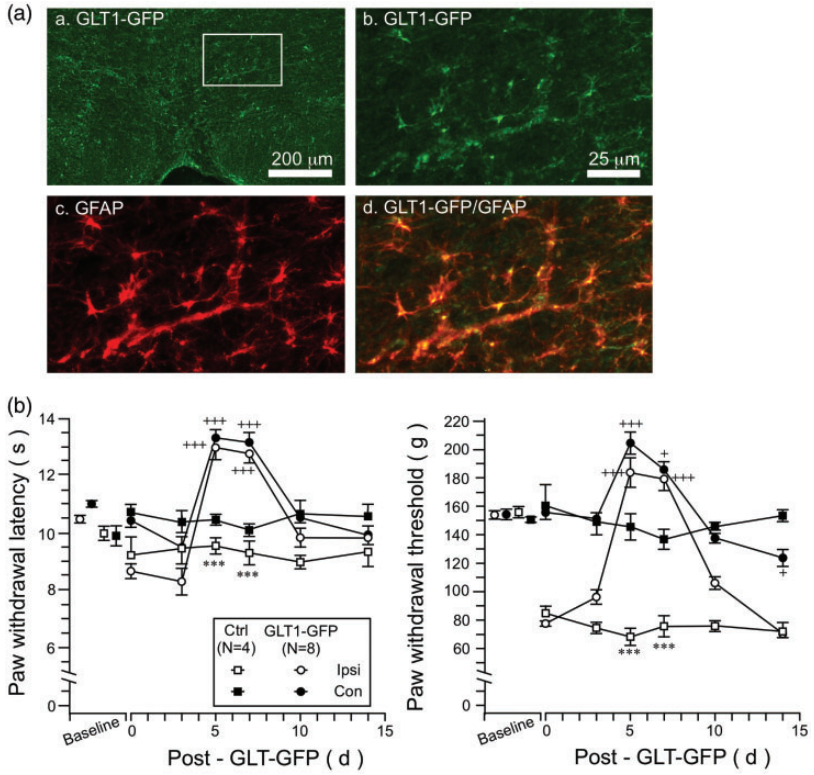

Figure 5. The effect of GLT1 overexpression on CFA-induced hyperalgesia. (A) GLT1-GFP immunostaining in the RVM. (a) Low power image of GLT1-GFP immunostaining. The area in the rectangle is enlarged in (b) to (d). (b) GLT1-GFP staining in high power. (c) GFAP immunostaining. (d) Double immunofluorescence labeling of GLT1-GFP and GFAP illustrating astroglial expression of transfected GLT1-GFP. (B) GLT1-GFP plasmid was transfected into the RVM at four weeks after CFA and its effect on behavioral hyperalgesia was assessed. GLT1 overexpression led to an increase in PWLs (Left) and PW threshold (Right) in both hind paws at five and seven days after gene transfer (Left). Note reversal of hyperalgesia on the inflamed paw. ***$p < 0.001$ vs. ctrl; $^{+}p < 0.05$; $^{+++}p < 0.001$ vs. four-week post-CFA (Day 0). GLT1: glutamate type 1 transporter; GFAP: glial fibrillary acidic protein; GFP: green fluorescent protein.

prevented upregulation of GLT1 and KBBP (Figure 7 (a)), suggesting that inflammation-induced GLT1/KBBP upregulation was dependent on input from the injured site. CFA induces rapid activation/phosphorylation of the extracellular signal-regulated kinase (ERK), mitogen-activated protein kinase (MAPK) in the RVM (Figure 7(b)).[59] pERK appeared in RVM neurons, but not astroglial cells, after inflammation (Figure 7(c)). At 30 min after the injection of CFA, phosphor-ERK (P44/42) exhibited significant upregulation in the RVM (not shown). Intra-RVM pretreatment (10 min before CFA) with PD98059 (50 ng), a MAPK kinases inhibitor, blocked CFA-induced upregulation of pERK as well as upregulation of GLT1 at 30 min after CFA (Figure 7(d)), further confirming a role of neuronal activity in altered GLT1.

We then studied the effect of early pharmacological block of GLT1 on the development of pain hypersensitivity. Dihydrokainate (10 ng) was injected into the RVM at 10 min prior to the injection of CFA. At 20 min after CFA, rats receiving DHK showed significantly shorter PWLs and lower PW threshold ($p < 0.001$) (Figure 7(e) and (f)), suggesting earlier development of pain hypersensitivity. These results suggest that GLT1 expression is regulated by neuronal input. The increased GLT1 activity immediately after inflammation may serve to enhance glutamate uptake, which counteracts increased synaptic activity and dampens the development of hyperalgesia.

Discussion

GLT1 plays a predominant role in maintaining glutamate homeostasis in the brain. Here, we have tested the hypothesis that changes in GLT1 activity in the brainstem descending circuitry contribute to the transition to persistent hyperalgesia. Following hind paw inflammation, we have identified initial transient upregulation of GLT1 expression in the RVM that was gradually transitioned to long-lasting downregulation. A delayed lasting downregulation of GLAST, the other major GLT, but not neuronal glutamate transporter EAAC1, was also observed. Similar biphasic changes of GLT expression have been observed at the

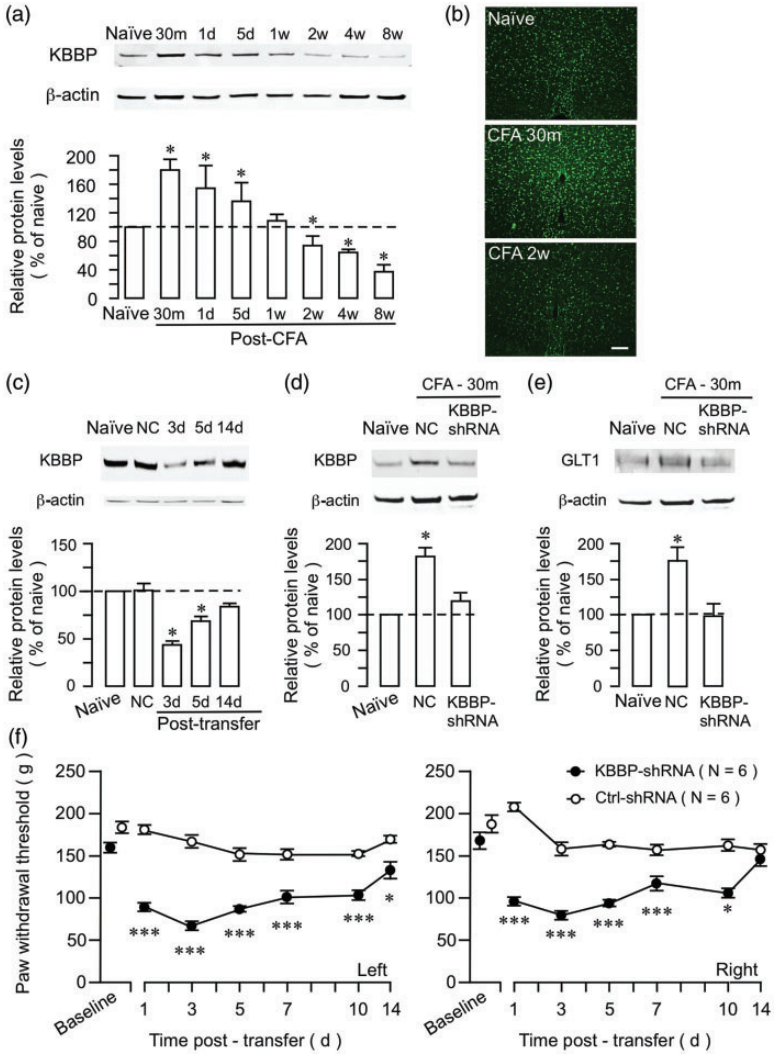

Figure 6. Altered KBBP expression in the RVM after hind paw inflammation and the effect of KBBP knock down on GLT1 and nociception. (a) Western immunoblot illustrating CFA-induced changes in KBBP expression. The RVM tissues were punched out at 30 min to eight weeks after CFA injection. *$p < 0.05$ vs. naïve. $N = 4$ for each time point. Error bars represent S.E.M. (b) KBBP immunostaining in the RVM was increased at 30 min and decreased at two weeks after CFA injection. (c) The KBBP protein levels in the RVM were downregulated at three to five days and recovered at 14 d after transfer of KBBP-shRNA. NC shRNA. *$p < 0.05$ vs. naïve. $N = 4$. KBBP (d) and GLT1 (e) protein levels in the RVM were upregulated at 30 min after CFA. The upregulation of both KBBP and GLT1 was abolished after the KBBP-shRNA treatment. (f) The PW thresholds of both left and right hind paws were significantly decreased at 1 to 10 days after the transfer of KBBP-shRNA, compared to rats receiving negative control-shRNA. *$p < 0.05$; ***$p < 0.001$ vs. Ctrl-shRNA. CFA: complete Freund's adjuvant; KBBP: kappa B-motif binding phosphoprotein; NC: negative control.

spinal level in other pain conditions[27,33] and in the brain in disease models such as epilepsy.[23] The significance of these changes, however, is not completely understood.

The rather peculiar temporal profile of GLT1 expression after inflammation, particularly a lasting late downregulation, led us to reevaluate the time course of CFA-induced behavioral hyperalgesia in rats. Extending previous reports,[40,46,60–62] we found that CFA-induced inflammatory hyperalgesia, as revealed by increased mechanical sensitivity and conditioned avoidance behavior, lasted much longer than previously reported (but see Weyer et al.[63]). Interestingly, a mild edema also seen throughout the observation period, suggesting sustained primary afferent input. Further analysis revealed that mechanical hyperalgesia exhibited an initial *developing* phase with peak hyperalgesia at 4 to 24 h and a subsequent *attenuating* phase with hyperalgesia gradually reducing toward the baseline, followed by a late *persistent* phase that lasted for months after inflammation (Figure 8). The thermal hyperalgesia showed similar *developing* and *attenuating* phases but was resolved after four weeks after CFA. Thus, CFA-induced mechanical hyperalgesia lasted longer than thermal hyperalgesia, which have been reported previously.[60,64]

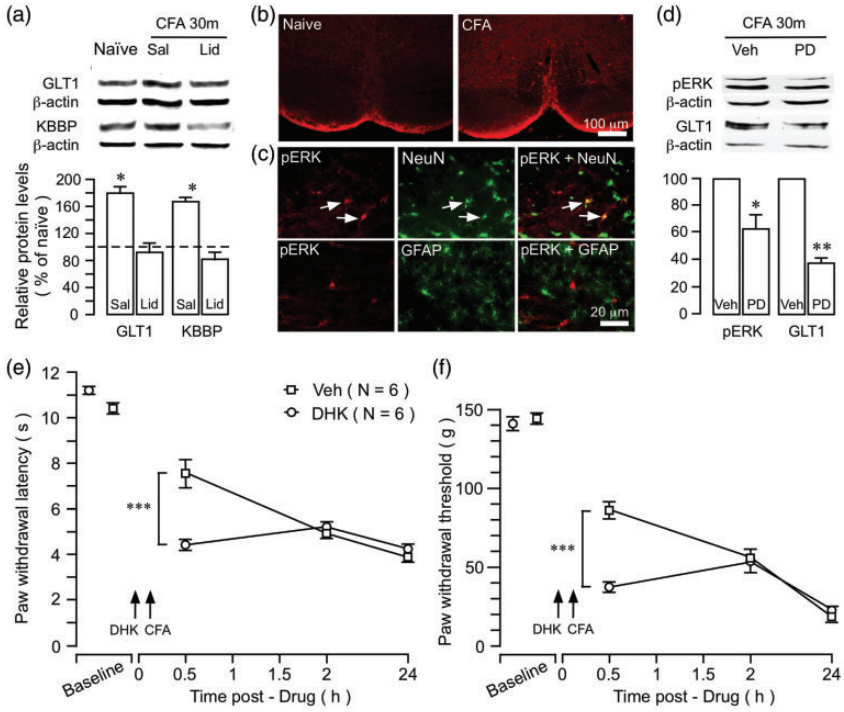

Figure 7. Significance of early upregulation of GLT1. (a) The effect of preemptive local anesthesia on inflammation-induced increase in GLT1. Lidocaine (Lid, 0.3 ml, 2%) was injected into the plantar surface of the hind paw 10 min prior to CFA injection into the same site. Saline (Sal, 0.3 ml, 0.9%) was injected as a control for lidocaine. The upregulation of both GLT1 and KBBP was prevented by local anesthetic block. *$p < 0.05$ vs. naïve and lidocaine, $N = 4$. (b) CFA-induced activation of ERK MAPK in the RVM. Examples of immunofluorescence staining illustrating inflammation-induced increase in pERK in the RVM. CFA was injected into one hind paw and the rat was perfused at 30 min after CFA. (c) Double immunofluorescence staining shows that CFA-induced pERK colocalized with NeuN, a neuronal marker, but not with GFAP, an astroglial marker. Arrows indicate examples of double-labeled neurons. (d) Intra-RVM injection of PD98059 (PD, 50 ng), a MAPK kinases inhibitor, attenuated CFA-induced upregulation of pERK and GLT1. *$p < 0.05$ vs. naïve or Veh, $N = 4$. Intra-RVM injection of DHK (10 ng), a selective GLT1 inhibitor, produced a further reduction of PWL (e) and PW threshold (f) in the inflamed paw at 20 min after CFA. ***$p < 0.001$ vs. Veh. CFA: complete Freund's adjuvant; GFAP: glial fibrillary acidic protein; DHK: dihydrokainic acid.

We noticed that using the plantar probe approach, CFA-induced mechanical hyperalgesia is resolved in 21 days in rats[65] and 10 days in mice.[66] Our dorsal probing approach may facilitate identifying weak hyperalgesia that could be masked by constitutive activity of opioid receptors.[65,66]

Reevaluation of the time course of CFA-induced inflammation and hyperalgesia offers an explanation for altered GLT1 in RVM with regard to the development of inflammatory pain (Figure 8). During the initial *developing* phase of hyperalgesia, GLT1 expression was rapidly upregulated as early as 30 min after inflammation. Similarly, KBBP and GFAP expression was also significantly increased. The early increase in GLT1 was suppressed by local anesthetic block of the injured site, suggesting a role of intense neural input after CFA injection. The increased GLT1 expression/activity early after injury may serve to enhance glutamate uptake and counteract increased synaptic activity. This view is supported by a delayed hyperalgesia or descending facilitation in vehicle-treated rats compared to rats pretreated with the GLT1 antagonist. However, this increase in GLT1 activity, as suggested by decreased nitration, is not sufficient to prevent the development of hyperalgesia, which is initiated by strong peripheral input. In the *attenuating* phase, GLT1 activity likely contributes to attenuation of hyperalgesia as injury-related input dampens, as indicated by nociceptive facilitation by DHK at one week after inflammation. However, GLT1 activity continues to decrease, as suggested by a gradual decrease in its expression and increased nitration. In the *persistent* phase, the further downregulation of GLT1 activity disrupts glutamate homeostasis and tilts the net descending modulation into a facilitatory state, contributing to the transition to persistent hyperalgesia. Okubo et al.[2] showed that the maintenance of secondary hyperalgesia involves a transition from peripheral to central descending mechanisms. Our findings are consistent with a role of the RVM circuitry in the transition from transient to persistent pain, involving GLT1.

Our results further support neuron–glial interactions in pain mechanisms. Modulation of RVM GLT1 by

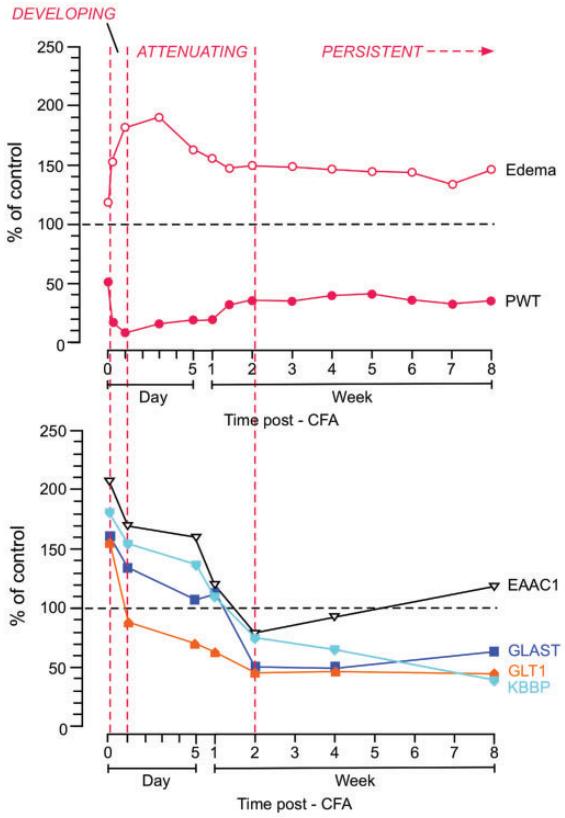

Figure 8. Correlation of the time courses of different end points after inflammation. The time courses of PWT and paw thickness (edema) (top) and glutamate transporters and KBBP (bottom) are compared. The time course is divided into the *DEVELOPING* (0-24h), *ATTENUATING* (one day to two weeks), and *PERSISTENT* (two-week) phases after the injection of CFA. The first point is 30 min after CFA. Note that downregulation of glutamate receptors GLT1, GLAST, and KBBP from two weeks correlates with the start of the persistent phase of mechanical hypersensitivity and edema. The neuronal glutamate transporter EAAC1 shows early upregulation and returned to the control level after the two-week time point. CFA: complete Freund's adjuvant; PWT: paw withdrawal threshold; KBBP: kappa B-motif binding phosphoprotein; GLT1: glutamate type 1 transporter.

peripheral inflammation depends on injury-related neural input, as indicated by our local anesthetic block experiment. KBBP, the transcriptional modulator of GLT1, exhibited similar biphasic changes after inflammation and was also sensitive to local anesthetic block. RNAi of GLT1 and KBBP similarly facilitated nocifensive responses and induced GLT1 expression reversed hyperalgesia. These results are consistent with the hypothesis that peripheral injury induces pain hypersensitivity involving neuron–glial interactions in the pain modulatory circuitry.[17] These interactions involve pre- and postsynaptic sites, microglia and astroglia, and inflammatory mediators.[67] Yan et al.[68,69] showed that release of IL-1β from microglia leads to decreased astro GLT activity and reduction of glutamate-glutamine cycle-dependent GABA synthesis in presynaptic neurons, followed by decreased GABAergic inhibition in the spinal dorsal horn. Consistently, IL-1β is induced in the RVM after nerve or tissue injury.[17,70]

GLT1 is almost exclusively localized to astroglia and enriched in their perisynaptic membranes,[20,32,71] (but also see Mennerick et al.[72]) although minor distribution of GLT1 is observed on axon terminals and their role in glutamate homeostasis cannot be completely excluded.[20,73] Astrocytes are activated in the RVM after peripheral tissue injury.[74] Neuronal input controls expression of GLT1 in astroglia[75] and is both necessary and sufficient to induce astroglial GLT1.[25] However, the neuron–astroglial interactions and GLT1 expression are complex. Reactive astrocytosis, as indicated by GFAP upregulation, does not parallel altered GLT1 expression after inflammation. In vitro studies show that activated astrocytes exhibit a "de-differentiated" phenotype with reduced GLT1 expression and that glial modulator propentofylline can induce GLT1 expression and glutamate uptake in activated astrocyte cultures.[76] It would be interesting to determine whether inflammation-induced GLT1 downregulation involves epigenetic mechanisms.[77,78] Yang et al.[79] show that GLT1 promoter can be suppressed by hypermethylation on selective CpG sites of the GLT1 promoter. We noted that upregulation of KBBP lasted longer than that of GLT1. We speculate that inflammation-induced epigenetic suppression of GLT1 expression may offset the effect of KBBP.

Downregulation of GLT1 is accompanied by reduced glial glutamate uptake from the synaptic cleft. In the neonatal neocortex, reduced astrocytic glutamate uptake has minimal effect on neuronal NMDA receptor activation.[80] Nevertheless, Nie and Weng[35] showed at the spinal level that increased synaptic glutamate could spill over to activate extrasynaptic GluN2B receptors, contributing to spinal hyperexcitability and pain. This mechanism may be applicable to the RVM. However, the RVM exerts both facilitatory and inhibitory influences, and the net effect of descending modulation is determined by multiple factors. For example, astroglial GABA transporters are involved in removing GABA, an inhibitory amino acid transmitter, from GABAergic terminals. After hind paw inflammation, the GABA transporter GAT expression was upregulated in the RVM (unpublished observations). The increased expression of GAT may facilitate removal of GABA and lead to a reduced GABAergic inhibition. In the RVM, removing GABA inhibition may disinhibit OFF-cells that produce descending inhibition.[14] Previous studies have examined the role of excitatory amino acid transmission in the RVM in descending pain modulation. Consistent with biphasic pain modulation, RVM glutamate receptors are involved in both pain facilitation and inhibition.[81–83] It is likely that glutamate homeostasis,

modulated and maintained at an appropriate level under normal conditions, is disrupted by injury. As the altered glutamate homeostasis persists, *net* descending facilitation follows and there is emergence of the *persistent* phase of CFA-induced hyperalgesia.

Pharmacological block and RNAi of GLT1/KBBP and GLT1 overexpression produced an effect on nocifensive behavior on both hind paws, which is consistent with a role of the RVM, a midline structure, in regulating pain without laterality.[19,84] Thus, once the RVM gets involved, one would expect to see hyperalgesia remote to the injured site. Mirror-image pain is observed in humans[85–89] and contralateral hyperalgesia develops after tissue[19,61,90,91]; and nerve[92,93] injury in animal models. We did not observe contralateral thermal hyperalgesia after inflammation but did see a significant mechanical hyperalgesia at the time when ipsilateral hyperalgesia peaked. Selective contralateral mechanical but not thermal hyperalgesia has been reported.[61,94] Studies have suggested that different neural mechanisms underlie thermal and mechanical hyperalgesia. [95–97] A subpopulation of RVM GABAergic neurons projecting to the spinal dorsal horn selectively inhibited mechanical nociception but had no effect on thermal pain sensitivity.[98] Nevertheless, the involvement of GLT1 in the transition from the *attenuating* to the *persistent* phase of mechanical hyperalgesia provides a model to study the central mechanisms of chronic pain. Strategies targeting at returning descending circuitry to homeostasis could be considered for managing chronic pain.

Acknowledgments

The authors would like to thank Dr J. Rothstein for providing the GLT1-GFP plasmid, Dr Y Yang and Dr H Misono for advice on GLT1 experiment and Dr M. Gu for helping with immunohistochemistry.

Author contributions

WG was involved in conception and design, collection and assembly of behavioral and Western blot data, data analysis and interpretation, and manuscript writing; SI contributed to conception and design, RNAi experiments, data analysis, and interpretation; SZ and JY were involved in collection and assembly of behavioral data; MW and JW were involved in collection and assembly of immunohistochemistry data; RD contributed to conception and design, data analysis and interpretation, and manuscript writing; FW contributed to conception and design, data analysis and interpretation, and manuscript writing; KR was involved in conception and design, assembly of data, data analysis and interpretation, and manuscript writing. All authors gave final approval of the manuscript.

Declaration of Conflicting Interests

The author(s) declared no potential conflicts of interest with respect to the research, authorship, and/or publication of this article.

Funding

The author(s) disclosed receipt of the following financial support for the research, authorship, and/or publication of this article: This work was supported by the National Institutes of Health (NS060735 and DE025137 to KR, DE018573 to FW, and DE021804 to RD). MW was supported by Grant-in-Aid for Scientific Research (No. 22592039) from the Japanese Ministry of Education, Science and Culture. JW was supported by the National Natural Science Foundation of China (No. 81371230).

Supplemental Material

Supplemental material for this article is available online.

References

1. Woolf CJ and Salter MW. Neuronal plasticity: Increasing the gain in pain. *Science* 2000; 288: 1765–1768.
2. Okubo M, Castro A, Guo W, Zou S, Ren K, Wei F, Keller A and Dubner R. Transition to persistent orofacial pain after nerve injury involves supraspinal serotonin mechanisms. *J Neurosci* 2013; 33: 5152–5161.
3. Garcia-Larrea L and Peyron R. Pain matrices and neuropathic pain matrices: a review. *Pain* 2013; 154: S29–S43.
4. Chapman CR and Vierck CJ. The transition of acute postoperative pain to chronic pain: an integrative overview of research on mechanisms. *J Pain* 2017; 18: 359.e1–359.e38.
5. Guo W, Robbins MT, Wei F, Zou S, Dubner R and Ren K. Supraspinal brain-derived neurotrophic factor signaling: a novel mechanism for descending pain facilitation. *J Neurosci* 2006; 26: 126–137.
6. Ren K and Dubner R. Descending control mechanisms. In: Basbaum AI, Kaneko A, Shepherd GM and Westheimer G (eds) *The senses: a comprehensive reference* (Vol. 5, *Pain*, Bushnell MC and Basbaum AI (eds)). San Diego: Academic Press, 2008, pp.723–762.
7. Heinricher MM, Tavares I, Leith JL and Lumb BM. Descending control of nociception: specificity, recruitment and plasticity. *Brain Res Rev* 2009; 60: 214–225.
8. Beitz AJ. The organization of afferent projections to the midbrain periaqueductal gray of the rat. *Neuroscience* 1982; 7: 133–159.
9. Jasmin L, Rabkin SD, Granato A, Boudah A and Ohara PT. Analgesia and hyperalgesia from GABA-mediated modulation of the cerebral cortex. *Nature* 2003; 424: 316–320.
10. Kong J, Tu PC, Zyloney C and Su TP. Intrinsic functional connectivity of the periaqueductal gray, a resting fMRI study. *Behav Brain Res* 2010; 211: 215–219.
11. Rizvi TA, Ennis M, Behbehani MM and Shipley MT. Connections between the central nucleus of the amygdala

and the midbrain periaqueductal gray: topography and reciprocity. *J Comp Neurol* 1991; 303: 121–131.
12. McGaraughty S, Farr DA and Heinricher MM. Lesions of the periaqueductal gray disrupt input to the rostral ventromedial medulla following microinjections of morphine into the medial or basolateral nuclei of the amygdala. *Brain Res* 2004; 1009: 223–227.
13. Chen Q, Roeder Z, Li MH, Zhang Y, Ingram SL and Heinricher MM. Optogenetic evidence for a direct circuit linking nociceptive transmission through the parabrachial complex with pain-modulating neurons of the rostral ventromedial medulla (RVM). *eNeuro* 2017; 4: pii: ENEURO.0202-17.2017.
14. Fields HL, Basbaum AI and Heinricher MM. Central nervous system mechanisms of pain modulation. In: McMahon S and Koltzenburg M (eds) *Wall and Melzack's textbook of pain*. 5th ed. London: Elsevier, 2006, pp.125–142.
15. Martins I and Tavares I. Reticular formation and pain: the past and the future. *Front Neuroanat* 2017; 11: 51.
16. Porreca F, Ossipov MH and Gebhart GF. Chronic pain and medullary descending facilitation. *Trends Neurosci* 2002; 25: 319–325.
17. Wei F, Guo W, Zou S, Ren K and Dubner R. Supraspinal glial-neuronal interactions contribute to descending pain facilitation. *J Neurosci* 2008; 28: 10482–10495.
18. Zhang W, Gardell S, Zhang D, Xie JY, Agnes RS, Badghisi H, Hruby VJ, Rance N, Ossipov MH, Vanderah TW, Porreca F and Lai J. Neuropathic pain is maintained by brainstem neurons co-expressing opioid and cholecystokinin receptors. *Brain* 2009; 132: 778–787.
19. Chai B, Guo W, Wei F, Dubner R. and Ren K Trigeminal-rostral ventromedial medulla circuitry is involved in orofacial hyperalgesia contralateral to tissue injury. *Mol Pain* 2012; 8: 78.
20. Danbolt NC. Glutamate uptake. *Prog Neurobiol* 2001; 65: 1–105.
21. Tao YX, Gu J and Stephens RL Jr. Role of spinal cord glutamate transporter during normal sensory transmission and pathological pain states. *Mol Pain* 2005; 1: 30.
22. Danbolt NC, Zhou Y, Furness DN and Holmseth S. Strategies for immunohistochemical protein localization using antibodies: what did we learn from neurotransmitter transporters in glial cells and neurons. *Glia* 2016; 64: 2045–2064.
23. Hubbard JA, Szu JI, Yonan JM and Binder DK. Regulation of astrocyte glutamate transporter-1 (GLT1) and aquaporin-4 (AQP4) expression in a model of epilepsy. *Exp Neurol* 2016; 283: 85–96.
24. Tanaka K, Watase K, Manabe T, Yamada K, Watanabe M, Takahashi K, Iwama H, Nishikawa T, Ichihara N, Kikuchi T, Okuyama S, Kawashima N, Hori S, Takimoto M and Wada K. Epilepsy and exacerbation of brain injury in mice lacking the glutamate transporter GLT-1. *Science* 1997; 276: 1699–1702.
25. Yang Y, Gozen O, Watkins A, Lorenzini I, Lepore A, Gao Y, Vidensky S, Brennan J, Poulsen D, Won Park J, Li Jeon N, Robinson MB and Rothstein JD. Presynaptic regulation of astroglial excitatory neurotransmitter transporter GLT1. *Neuron* 2009; 61: 880–894.
26. Ren K. Emerging role of astroglia in pain hypersensitivity. *Jpn Dent Sci Rev* 2010; 46: 86–92.
27. Sung B, Lim G and Mao J. Altered expression and uptake activity of spinal glutamate transporters after nerve injury contribute to the pathogenesis of neuropathic pain in rats. *J Neurosci* 2003; 23: 2899–2910.
28. Binns BC, Huang Y, Goettl VM, Hackshaw KV and Stephens RL Jr. Glutamate uptake is attenuated in spinal deep dorsal and ventral horn in the rat spinal nerve ligation model. *Brain Res* 2005; 1041: 38–47.
29. Weng HR, Aravindan N, Cata JP, Chen JH, Shaw AD and Dougherty PM. Spinal glial glutamate transporters down-regulate in rats with taxol-induced hyperalgesia. *Neurosci Lett* 2005; 386: 18–22.
30. Cavaliere C, Cirillo G, Rosaria Bianco M, Rossi F, D, Novellis V, Maione S and Papa M. Gliosis alters expression and uptake of spinal glial amino acid transporters in a mouse neuropathic pain model. *Neuron Glia Biol* 2007; 3: 141–153.
31. Wang W, Wang W, Wang Y, Huang J, WU S and Li YQ. Temporal changes of astrocyte activation and glutamate transporter-1 expression in the spinal cord after spinal nerve ligation-induced neuropathic pain. *Anat Rec* 2008; 291: 513–518.
32. Xin WJ, Weng HR and Dougherty PM. Plasticity in expression of the glutamate transporters GLT-1 and GLAST in spinal dorsal horn glial cells following partial sciatic nerve ligation. *Mol Pain* 2009; 5: 15.
33. Mirzaei V, Manaheji H, Maghsoudi N and Zaringhalam J. Comparison of changes in mRNA expression of spinal glutamate transporters following induction of two neuropathic pain models. *Spinal Cord* 2010; 48: 791–797.
34. Yaster M, Guan X, Petralia RS, Rothstein JD, Lu W and Tao YX. Effect of inhibition of spinal cord glutamate transporters on inflammatory pain induced by formalin and complete Freund's adjuvant. *Anesthesiology* 2011; 114: 412–423.
35. Nie H and Weng HR. Impaired glial glutamate uptake induces extrasynaptic glutamate spillover in the spinal sensory synapses of neuropathic rats. *J Neurophysiol* 2010; 103: 2570–2580.
36. Liaw WJ, Stephens RL Jr, Binns BC, Chu Y, Sepkuty JP, Johns RA, Rothstein JD and Tao YX. Spinal glutamate uptake is critical for maintaining normal sensory transmission in rat spinal cord. *Pain* 2005; 115: 60–70.
37. Weng HR, Chen JH and Cata JP. Inhibition of glutamate uptake in the spinal cord induces hyperalgesia and increased responses of spinal dorsal horn neurons to peripheral afferent stimulation. *Neuroscience* 2006; 138: 1351–1360.
38. Ramos KM, Lewis MT, Morgan KN, Crysdale NY, Kroll JL, Taylor FR, Harrison JA, Sloane EM, Maier SF and Watkins LR. Spinal upregulation of glutamate transporter GLT-1 by ceftriaxone: therapeutic efficacy in a range of experimental nervous system disorders. *Neuroscience* 2010; 169: 1888–1900.
39. Yang M, Roman K, Chen DF, Wang ZG, Lin Y and Stephens RL Jr. GLT-1 overexpression attenuates bladder nociception and local/cross-organ sensitization of bladder nociception. *Am J Physiol Renal Physiol* 2011; 300: F1353–F1359.

40. Iadarola MJ, Douglass J, Civelli O and Naranjo JR. Differential activation of spinal cord dynorphin and enkephalin neurons during hyperalgesia: evidence using cDNA hybridization. *Brain Res* 1988; 455: 205–212.
41. Hylden JLK, Nahin RL, Traub RJ and Dubner R. Expansion of receptive fields of spinal lamina I projection neurons in rats with unilateral adjuvant-induced inflammation: the contribution of dorsal horn mechanisms. *Pain* 1989; 37: 229–243.
42. Ren K, Hylden JLK, Williams GM, Ruda MA and Dubner R. The effects of a non-competitive NMDA receptor antagonist, MK-801, on behavioral hyperalgesia and dorsal horn neuronal activity in rats with unilateral inflammation. *Pain* 1992; 50: 331–344.
43. Guo W, Zou S-P, Guan Y, Ikeda T, Tal M, Dubner R and Ren K. Tyrosine phosphorylation of the NR2B subunit of the NMDA receptor in the spinal cord during the development and maintenance of inflammatory hyperalgesia. *J Neurosci* 2002; 22: 6208–6217.
44. Khodorova A, Zou S, Ren K, Dubner R, Davar G and Strichartz G. Dual roles for endothelin-B receptors in modulating adjuvant-induced inflammatory hyperalgesia in rats. *Open Pain J* 2009; 2: 30–40.
45. Hargreaves K, Dubner R, Brown F, Flores C and Joris J. A new and sensitive method for measuring thermal nociception in cutaneous hyperalgesia. *Pain* 1988; 32: 77–88.
46. Ren K. An improved method for assessing mechanical allodynia in the rat. *Physiol Behav* 1999; 67: 711–716.
47. LaBuda CJ and Fuchs PN. A behavioral test paradigm to measure the aversive quality of inflammatory and neuropathic pain in rats. *Exp Neurol* 2000; 163: 490–494.
48. Guo W, Chu YX, Imai S, Yang JL, Zou S, Mohammad Z, Wei F, Dubner R and Ren K. Further observations on the behavioral and neural effects of bone marrow stromal cells in rodent pain models. *Mol Pain* 2016; 12. pii: 1744806916658043. doi: 10.1177/1744806916658043.
49. Guo W, Wang H, Zou S, Gu M, Watanabe M, Wei F, Dubner R, Huang GT and Ren K. Bone marrow stromal cells produce long-term pain relief in rat models of persistent pain. *Stem Cells* 2011; 29: 1294–1303.
50. Paxinos P and Watson C. *The rat brain in stereotaxic coordinates*. 6th ed. New York: Academic Press, 2008.
51. Wei F, Dubner R, Zou S, Ren K, Bai G, Wei D and Guo W. Molecular depletion of descending serotonin unmasks its novel facilitatory role in the development of persistent pain. *J Neurosci* 2010; 30: 8624–8636.
52. Haugeto O, Ullensvang K, Levy LM, Chaudhry FA, Honoré T, Nielsen M, Lehre KP and Danbolt NC. Brain glutamate transporter proteins form homomultimers. *J Biol Chem* 1996; 271: 27715–27722.
53. Ji YF, Zhou L, Xie YJ, Xu SM, Zhu J, Teng P, Shao CY, Wang Y, Luo JH and Shen Y. Upregulation of glutamate transporter GLT–1 by mTOR-Akt-NF-κB cascade in astrocytic oxygen-glucose deprivation. *Glia* 2013; 61: 1959–1975.
54. Coleman E, Judd R, Hoe L, Dennis J and Posner P. Effects of diabetes mellitus on astrocyte GFAP and glutamate transporters in the CNS. *Glia* 2004; 48: 166–178.
55. Trotti D, Rossi D, Gjesdal O, Levy LM, Racagni G, Danbolt NC and Volterra A. Peroxynitrite inhibits glutamate transporter subtypes. *J Biol Chem* 1996; 271: 5976–5979.
56. Chen Z, Muscoli C, Doyle T, Bryant L, Cuzzocrea S, Mollace V, Mastroianni R, Masini E and Salvemini D. NMDA-receptor activation and nitroxidative regulation of the glutamatergic pathway during nociceptive processing. *Pain* 2010; 149: 100–106.
57. Al Awabdh S, Gupta-Agarwal S, Sheehan DF, Muir J, Norkett R, Twelvetrees AE, Griffin LD and Kittler JT. Neuronal activity mediated regulation of glutamate transporter GLT-1 surface diffusion in rat astrocytes in dissociated and slice cultures. *Glia* 2016; 64: 1252–1264.
58. Guan Y, Guo W, Robbins MT, Dubner R and Ren K. Changes in AMPA receptor phosphorylation in the rostral ventromedial medulla after inflammatory hyperalgesia in rats. *Neurosci Lett* 2004; 366: 201–205.
59. Imbe H, Kimura A, Okamoto K, Donishi T, Aikawa F, Senba E and Tamai Y. Activation of ERK in the rostral ventromedial medulla is involved in hyperalgesia during peripheral inflammation. *Brain Res* 2008; 1187: 103–110.
60. Millan MJ, Członkowski A, Morris B, Stein C, Arendt R, Huber A, Höllt V and Herz A. Inflammation of the hind limb as a model of unilateral, localized pain: influence on multiple opioid systems in the spinal cord of the rat. *Pain* 1988; 35: 299–312.
61. Gao YJ, Xu ZZ, Liu YC, Wen YR, Decosterd I and Ji RR. The c-Jun N-terminal kinase 1 (JNK1) in spinal astrocytes is required for the maintenance of bilateral mechanical allodynia under a persistent inflammatory pain condition. *Pain* 2010; 148: 309–319.
62. Zhang W, Liu LY and Xu TL. Reduced potassium-chloride co-transporter expression in spinal cord dorsal horn neurons contributes to inflammatory pain hypersensitivity in rats. *Neuroscience* 2008; 152: 502–510.
63. Weyer AD, Zappia KJ, Garrison SR, O'Hara CL, Dodge AK and Stucky CL. Nociceptor sensitization depends on age and pain chronicity(1,2,3). *eNeuro* 2016; 3: pii: ENEURO.0115-15.2015.
64. Ambalavanar R, Yallampalli C, Yallampalli U and Dessem D. Injection of adjuvant but not acidic saline into craniofacial muscle evokes nociceptive behaviors and neuropeptide expression. *Neuroscience* 2007; 149: 650–659.
65. Walwyn WM, Chen W, Kim H, Minasyan A, Ennes HS, McRoberts JA and Marvizón JC. Sustained suppression of hyperalgesia during latent sensitization by μ-, δ-, and κ-opioid receptors and α2A adrenergic receptors: role of constitutive activity. *J Neurosci* 2016; 36: 204–221.
66. Corder G, Doolen S, Donahue RR, Winter MK, Jutras BL, He Y, Hu X, Wieskopf JS, Mogil JS, Storm DR, Wang ZJ, McCarson KE and Taylor BK. Constitutive μ-opioid receptor activity leads to long-term endogenous analgesia and dependence. *Science* 2013; 341: 1394–1399.
67. Ren K and Dubner R. Activity-triggered tetrapartite neuron-glial interactions following peripheral injury. *Curr Opin Pharmacol* 2016; 26: 16–25.
68. Yan X, Yadav R, Gao M and Weng HR. Interleukin-1 beta enhances endocytosis of glial glutamate transporters in the spinal dorsal horn through activating protein kinase C. *Glia* 2014; 62: 1093–1109.

69. Yan X, Jiang E and Weng HR. Activation of toll like receptor 4 attenuates GABA synthesis and postsynaptic GABA receptor activities in the spinal dorsal horn via releasing interleukin-1 beta. *J Neuroinflammation* 2015; 12: 222.
70. Ren K. Exosomes in perspective: a potential surrogate for stem cell therapy. *Odontology*. Epub ahead of print 15 October 2018. DOI: 10.1007/s10266-018-0395-9.
71. Rothstein JD, Martin L, Levey AI, Dykes-Hoberg M, Jin L, Wu D, Nash N and Kuncl RW. Localization of neuronal and glial glutamate transporters. *Neuron* 1994; 13: 713–725.
72. Mennerick S, Dhond RP, Benz A, Xu W, Rothstein JD, Danbolt NC, Isenberg KE and Zorumski CF. Neuronal expression of the glutamate transporter GLT-1 in hippocampal microcultures. *J Neurosci* 1998; 18: 4490–4499.
73. Danbolt NC, Furness DN and Zhou Y. Neuronal vs glial glutamate uptake: resolving the conundrum. *Neurochem Int* 2016; 98: 29–45.
74. Roberts J, Ossipov MH and Porreca F. Glial activation in the rostroventromedial medulla promotes descending facilitation to mediate inflammatory hypersensitivity. *Eur J Neurosci* 2009; 30: 229–241.
75. Swanson RA, Liu J, Miller JW, Rothstein JD, Farrell K, Stein BA and Longuemare MC. Neuronal regulation of glutamate transporter subtype expression in astrocytes. *J Neurosci* 1997; 17: 932–940.
76. Tawfik VL, Lacroix-Fralish ML, Bercury KK, Nutile-McMenemy N, Harris BT and Deleo JA. Induction of astrocyte differentiation by propentofylline increases glutamate transporter expression in vitro: heterogeneity of the quiescent phenotype. *Glia* 2006; 54: 193–203.
77. Perisic T, Holsboer F, Rein T and Zschocke J. The CpG island shore of the GLT-1 gene acts as a methylation-sensitive enhancer. *Glia* 2012; 60: 1345–1355.
78. Bai G, Ren K and Dubner R. Epigenetic regulation of persistent pain. *Transl Res* 2015; 165: 177–199.
79. Yang Y, Gozen O, Vidensky S, Robinson MB and Rothstein JD. Epigenetic regulation of neuron-dependent induction of astroglial synaptic protein GLT1. *Glia* 2010; 58: 277–286.
80. Hanson E, Armbruster M, Cantu D, Andresen L, Taylor A, Danbolt NC and Dulla CG. Astrocytic glutamate uptake is slow and does not limit neuronal NMDA receptor activation in the neonatal neocortex. *Glia* 2015; 63: 1784–1796.
81. Urban MO, Coutinho SV and Gebhart GF. Involvement of excitatory amino acid receptors and nitric oxide in the rostral ventromedial medulla in modulating secondary hyperalgesia produced by mustard oil. *Pain* 1999; 81: 45–55.
82. Heinricher MM, Schouten JC and Jobst EE. Activation of brainstem N-methyl-D-aspartate receptors is required for the analgesic actions of morphine given systemically. *Pain* 2001; 92: 129–138.
83. Guan Y, Terayama R, Dubner R and Ren K. Plasticity in excitatory amino acid receptor-mediated descending pain modulation after inflammation. *J Pharmacol Exp Ther* 2002; 300: 513–520.
84. Hurley RW and Hammond DL. The analgesic effects of supraspinal mu and delta opioid receptor agonists are potentiated during persistent inflammation. *J Neurosci* 2000; 20: 1249–1259.
85. Maleki J, LeBel AA, Bennett GJ and Schwartzman RJ. Patterns of spread in complex regional pain syndrome, type I (reflex sympathetic dystrophy). *Pain* 2000; 88: 259–266.
86. Woda A and Pionchon P. A unified concept of idiopathic orofacial pain: pathophysiologic features. *J Orofac Pain* 2000; 14: 196–212.
87. Shenker NG, Haigh RC, Mapp PI, Harris N and Blake DR. Contralateral hyperalgesia and allodynia following intradermal capsaicin injection in man. *Rheumatology (Oxford)* 2008; 47: 1417–1421.
88. Huang D and Yu B. The mirror-image pain: an unclered phenomenon and its possible mechanism. *Neurosci Biobehav Rev* 2010; 34: 528–532.
89. Kang K, Lee JH and Kim HG. Contralateral referred pain in a patient with intramedullary spinal cord metastasis from extraskeletal small cell osteosarcoma. *J Spinal Cord Med* 2013; 36: 695–699.
90. Raghavendra V, Tanga FY and DeLeo JA. Complete Freund's adjuvant-induced peripheral inflammation evokes glial activation and proinflammatory cytokine expression in the CNS. *Eur J Neurosci* 2004; 20: 467–473.
91. Ambalavanar R, Moutanni A and Dessem D. Inflammation of craniofacial muscle induces widespread mechanical allodynia. *Neurosci Lett* 2006; 399: 249–254.
92. Koltzenburg M, Wall PD and McMahon SB. Does the right side know what the left is doing?. *Trends Neurosci* 1999; 22: 122–127.
93. Milligan ED, Twining C, Chacur M, Biedenkapp J, O'Connor K, Poole S, Tracey K, Martin D, Maier SF and Watkins LR. Spinal glia and proinflammatory cytokines mediate mirror-image neuropathic pain in rats. *J Neurosci* 2003; 23: 1026–1040.
94. Nagakura Y, Okada M, Kohara A, Kiso T, Toya T, Iwai A, Wanibuchi F and Yamaguchi T. Allodynia and hyperalgesia in adjuvant-induced arthritic rats: time course of progression and efficacy of analgesics. *J Pharmacol Exp Ther* 2003; 306: 490–497.
95. Abbadie C, Lindia JA, Cumiskey AM, Peterson LB, Mudgett JS, Bayne EK, DeMartino JA, MacIntyre DE and Forrest MJ. Impaired neuropathic pain responses in mice lacking the chemokine receptor CCR2. *Proc Natl Acad Sci U S A* 2003; 100: 7947–7952.
96. Thacker MA, Clark AK, Bishop T, Grist J, Yip PK, Moon LD, Thompson SW, Marchand F and McMahon SB. CCL2 is a key mediator of microglia activation in neuropathic pain states. *Eur J Pain* 2009; 13: 263–272.
97. Yang CJ, Wang XW, Li X, Wu GC, Wang YQ and Mao-Ying QL. A rat model of bone inflammation-induced pain by intra-tibial complete Freund's adjuvant injection. *Neurosci Lett* 2011; 490: 175–179.
98. François A, Low SA, Sypek EI, Christensen AJ, Sotoudeh C, Beier KT, Ramakrishnan C, Ritola KD, Sharif-Naeini R, Deisseroth K, Delp SL, Malenka RC, Luo L, Hantman AW and Scherrer G. A brainstem-spinal cord inhibitory circuit for mechanical pain modulation by GABA and enkephalins. *Neuron* 2017; 93: 822–839.